INVITED PAPER *Special Section on Recent Progress in Physics and Applications of Intrinsic Josephson Junctions*

Terahertz Radiations and Switching Phenomena of Intrinsic Josephson Junctions in High-Temperature Superconductors: Josephson Phase Dynamics in Long- and Short-Ranged Interactions

Itsuhiro KAKEYA[†a)], ***Nonmember***

SUMMARY Studies on intrinsic Josephson junctions (IJJs) of cuprate superconductors are reviewed. A system consisting of a few IJJs provides phenomena to test the Josephson phase dynamics and its interaction between adjacent IJJs within a nanometer scale, which is unique to cuprate superconductors. Quasiparticle density of states, which provides direct information on the Cooper-pair formation, is also revealed in the system. In contrast, Josephson plasma emission, which is an electromagnetic wave radiation in the sub-terahertz frequency range from an IJJ stack, arises from the synchronous phase dynamics of hundreds of IJJs coupled globally. This review summarizes a wide range of physical phenomena in IJJ systems having capacitive and inductive couplings with different nanometer and micrometer length scales, respectively.

key words: *intrinsic Josephson junction, macroscopic quantum tunneling, Josephson critical current, terahertz radiation, synchronous oscillation*

1. Introduction

In July 1992, at the third International Conference on Materials and Mechanisms in High-Temperature Superconductors (M2S-HTSC III) held in Kanazawa, Japan, two important breakthroughs on electrical conductivity in high-T_c superconductors were presented. The first breakthrough was presented by R. Kleiner, a researcher from Professor Paul Müller's group at Walter Meissner Institute, Germany [1]. The second one was presented by Professor Ginichiro Oya's group at Utsunomiya University [2]. Both reported the peculiarity of the c-axis conduction in $Bi_2Sr_2CaCu_2O_{8+\delta}$ (Bi2212) single crystals and pointed out that it can be described by the Josephson effect. Subsequent studies also revealed that in copper oxide superconductors, the superconducting electron pairs are generally localized in the CuO_2 layer, and the c-axis electrical conduction is described by the Josephson effect that arises out of the alternative stacking of CuO_2 and insulating atomic layers [3]. Thus, Josephson junctions originating from the localization of superconducting electron pairs in superconductors with layered crystal structures, including organic and iron-based superconductors, are designated as intrinsic Josephson junctions (IJJs). As bismuth based superconductors with large anisotropy can extract individual properties of IJJs and have an ideal tunnel barrier for Josephson junctions, researchers worldwide have been studying IJJs in bismuth-based high-T_c superconductors. Particularly characteristic phenomena are the multi-branched current–voltage characteristics, the quasiparticle spectrum directly indicating the superconducting gap [4], [5], electromagnetic absorption called Josephson plasma resonance [6]–[8], and the two-dimensional nature of vortex penetration [9]–[13]. These findings about the fundamental physical properties of the IJJ systems provide a basis for terahertz (THz) electromagnetic wave emission by coherent oscillation, which was later demonstrated in Refs. [14]–[25].

The variety of phenomena in an IJJ system is mainly attributed to the two coupling mechanisms between IJJs of different length scales: inductive and capacitive couplings. The inductive coupling originates from the current flowing within a superconducting layer (SL) [26]. Josephson vortices penetrating the adjacent block layer (BL) share their eddy currents, resulting in formation of a triangular or rectangular Josephson vortex lattice over the entire stack. The capacitive coupling is attributed to the breaking of the charge neutrality of an SL because the SL thickness is comparable to the Debye charge-screening length ($\sim$ 1 nm) [27]. The charged SL induces additional phase changes in the adjacent IJJs resulting in multi-branched current–voltage characteristics [28] and longitudinal Josephson plasma resonance [7].

In this paper, some important results of my research on IJJs are described from two aspects: simplified quasiparticle and phase dynamics for one or a few IJJs under short-range capacitive coupling between IJJs and complicated macroscopic phenomena in hundreds of coupled IJJs under long-range inductive coupling. The former is known as intrinsic tunneling spectroscopy [29], [30] or cooperative macroscopic quantum tunneling in IJJs [31]–[33]. The latter is the Josephson plasma emission in the terahertz frequency range by synchronous Josephson oscillation of the stacked IJJs [34]–[40].

2. Cooperative Quantum Tunneling in Single, Double, and Triple CuO_2 Plane IJJs

Superconductivity is a typical example of a macroscopic quantum phenomenon in which the wave nature of electrons appears macroscopically, and unusual phenomena are observed in the macroscopic world. One such interesting

Manuscript received July 19, 2022.
Manuscript revised October 22, 2022.
Manuscript publicized December 7, 2022.
[†]The author is with Graduate School of Engineering, Kyoto University, Kyoto-shi, 615–8510 Japan.
a) E-mail: kakeya@kuee.kyoto-u.ac.jp
DOI: 10.1587/transele.2022SEI0004

phenomenon is macroscopic quantum tunneling observed in Josephson junctions. The tunneling effect due to the Heisenberg uncertainty principle appears in fluctuations of current–voltage characteristics, and this phenomenon is the operating principle of quantum bits (qubits), which are used in quantum computing. We have succeeded in extracting phenomena originating from short-range interactions between intrinsic Josephson junctions in high-T_c superconductors. This is a breakthrough for using IJJs as qubits, which is considered technically challenging, and expected to lead toward the realization of a significantly less complicated quantum computer that does not require a dilution refrigerator [41]–[47].

To observe the quantum tunneling phenomena in IJJs, it is necessary to extract a small number of IJJs from a single crystal, which is a stack of thousands of IJJs and observe their switching dynamics. In our mesa structured device, it is essential to reduce the contact resistance of the electrode deposited on the surface of a single crystal to extract the IJJs, which makes it difficult to obtain a controlled number of IJJs. We focused on the fact that the resistance at the interface between the electrode and the Bi2212 single-crystal is caused by moisture in the air. Moreover, we cleaved the Bi2212 single–crystal in a vacuum to eliminate the annealing process, thereby enabling highly accurate control of the number of extracted IJJs [45], [48].

In the mesa device with a few IJJs thus obtained, the voltage switching characteristics of a specific IJJ switching from a zero-voltage state to a finite voltage state were measured at cryogenic temperatures of 0.4 K. The mesa structures were fabricated on single crystals of three different superconductors represented by $Bi_2Sr_2Ca_{n-1}Cu_nO_{2n+4+\delta}$, where we write Bi2201, Bi2212, and Bi2223 for $n = 1 - 3$, respectively. In these superconductors, we focused on the fact that the capacitive coupling can be varied as the period of the Josephson junction changes from 1.2, 1.5, to 1.8 nm as shown in Fig. 1 (a). The quantum fluctuations in the switching characteristics of the first junction at the top of the mesa structure and the second junction were evaluated. Figure 1 (b) shows the graph of effective temperature versus bath temperature for the switching current in the three materials. The effective temperature $T_{\rm eff}$ is evaluated by fluctuations of the switching current of the IJJs according to the Kramers' model as

$$\Gamma = \frac{\omega_p}{2\pi} \exp\left(-\frac{\Delta U}{k_B T_{\rm eff}}\right), \qquad (1)$$

where Γ is the thermal escape rate measured by zero-to-finite resistance switching fluctuation of the IJJ, ω_p is the Josephson plasma frequency, and ΔU is the barrier potential of the washboard model [49].

In Bi2223, where the two IJJs are relatively far apart because of a CuO_2 inner plane, the quantum fluctuations of both junctions are almost equivalent. This contrasts with the results for Bi2212 and Bi2201, where the quantum fluctuation of the second switching is significantly pronounced presumably because of the capacitive coupling between neighboring IJJs. This result can also be explained by the fact that in Bi2223, the triple CuO_2 planes form an SL, and the inner-plane of the CuO_2 triple layer interrupts the correlation between the Josephson junctions, considering that the observed superconducting tunneling current between the SLs is the Josephson current [31]–[33].

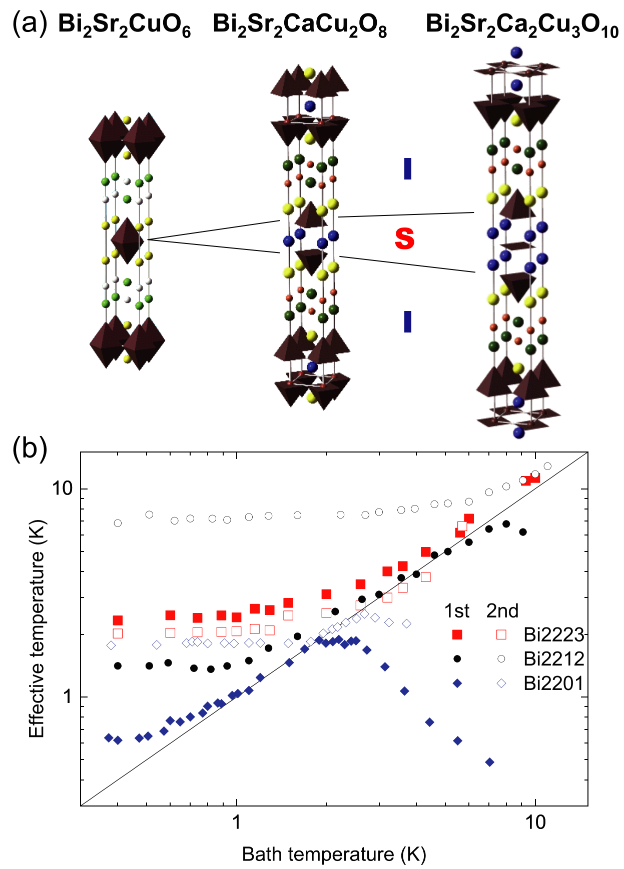

Fig. 1 (a) Crystal structures of Bi2201 (left), Bi2212 (center), and Bi2223 (right) where the superconducting electron is located at the atomic layers marked with S, forming a Josephson junction. (b) Temperature dependence of the switching fluctuation of the first (solid) and second (open) junctions in Bi2201, Bi2212, and Bi2223. where the quantum fluctuation observed at 0.4 K is more pronounced in the second junction than in the first junction.

3. Variation of Josephson Critical Current Density of Multi-Layered CuO_2 Planes

We have revealed a clear difference between Bi2212 with two CuO_2 atomic planes (T_c < 90K) and Bi2223 with three planes (T_c < 110K) through detailed examinations of the electrical resistance behavior at the superconducting transition and current–voltage characteristics in the superconducting state. This was achieved by developing a microfabrication technique that allows obtaining mesa structures with a thickness of less than 5 nm, consisting of a few IJJs. When a non-superconducting, normal-conductive metal is microscopically adhered to a superconductor by a vacuum deposition method, superconducting electrons penetrate the

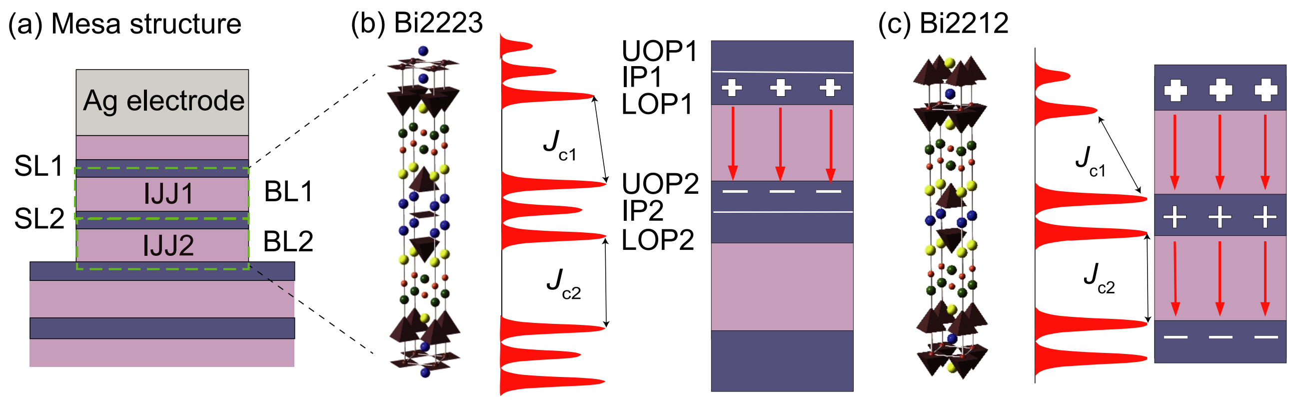

Fig. 2 (a) Cross-sectional schematic drawing of the mesa device with two IJJs. (b,c) Crystal structure and proposed distribution (red) of superconducting electrons of Bi2223 (b) and Bi2212 (c), which reproduce critical current measurements of the devices. A superconducting layer (SL) of Bi2223 consists of three CuO_2 planes, upper outer plane (UOP), inner-plane (IP), and lower outer plane (LOP). Charging of SLs is more pronounced in Bi2212; hence the capacitive coupling (red arrows) is more significant. Critical current density J_c is determined by a product of superconducting electron density of two OPs sandwiching a block layer (BL). Reproduced with permission from [33], copyright 2019 The American Physical Society.

normal-conductive metal. This proximity effect is significantly weaker in Bi2223 than in Bi2212, and the decay of the proximity effect is more significant than the increase in the SL thickness with increasing n. This can be explained by considering that the superconducting electrons are localized within the CuO_2 atomic planes rather than being uniformly distributed throughout the SL, which consists of multiple CuO_2 atomic planes as shown in Fig. 2.

The phenomena that can be explained by this model have also been observed in the phase tunneling phenomena in Josephson junctions. For $n = 1$ and 2, where the superconducting layers are thin, quantum tunneling was observed. This indicates a strong coupling of phase differences in adjacent junctions. On the other hand, for $n = 3$, strong coupling between adjacent junctions was not observed as discussed in the previous section [33]. Such example of a pronounced localization of superconducting electrons inside an SL has not been reported previously, and a detailed theory that incorporates the structure inside the SL is necessary to explain the intrinsic Josephson phenomenon in the future.

4. Intrinsic Tunneling Spectroscopy and Josephson Current in Cuprate Superconductors

Intrinsic tunneling spectroscopy (ITS) is a technique by which information on the quasiparticle density of states (DOS) in the CuO_2 layers can be extracted from the c-axis current–voltage characteristics [4]. Since an IJJ inside the crystal is protected by other IJJs, ITS probing allows access to the bulk quasiparticle DOS protected from surface deterioration. This contrasts with surface-sensitive spectroscopic methods, such as angle-resolved photoemission spectroscopy and scanning tunneling spectroscopy. The superconducting gap Δ, which is the coupling force of superconducting electron pairs, is revealed from the quasiparticle DOS. ITS enables the comparison of the measured

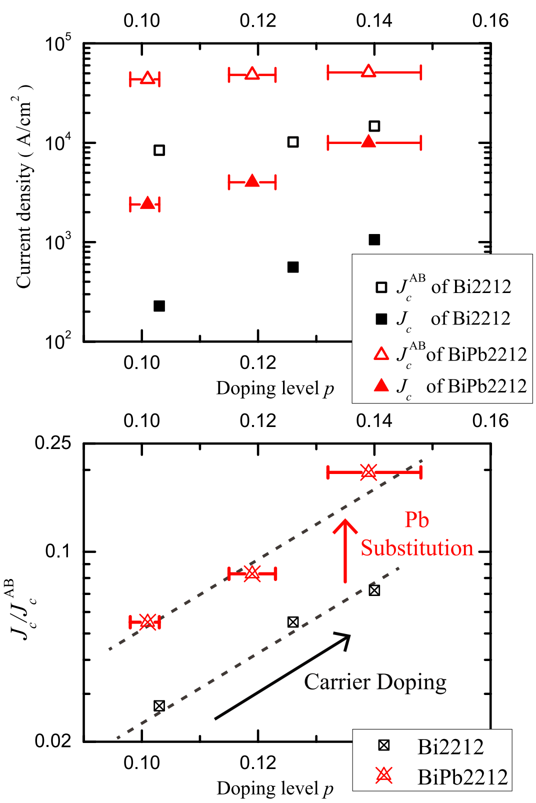

Fig. 3 Plots for J_c, J_c^{AB}, and J_c/J_c^{AB} as a function of doping p for BiPb2212 and Bi2212. Reproduced with permission from [29], copyright 2013 The American Physical Society.

Josephson critical current density J_c and the Ambegaokar–Baratoff-Josephson critical current J_c^{AB} in the same crystal using the following equation:

$$J_c^{AB} \simeq \frac{\pi\Delta}{2eR_NS}, \quad (2)$$

where R_N is the normal tunneling resistance, S is the area of the Josephson junction, and e is the elementary charge [50]. However, this relation does not hold for high-T_c cuprates presumably because of the partial filling of quasiparticle Fermi surface with respect to the d-wave superconducting gap in the momentum space (Fermi arc) [51].

We measured J_c and ITS in mesa-structured $Bi_{1.8}Pb_{0.2}Sr_2CaCu_2O_{8+\delta}$ (BiPb2212) single crystals and compared the results with those previously obtained in pristine Bi2212 crystals. Figure 3 shows the critical current densities in BiPb2212 and Bi2212 and the ratio J_c/J_c^{AB} in the same carrier doping range [52]. The carrier doping p was estimated from precise Hall-effect measurements in thin crystals with the identical nominal composition as the ITS measurements. In BiPb2212, J_c/J_c^{AB} is found to be twice that in Bi2212, suggesting that Fermi arc expands by partially substituting Bi by Pb in Bi2212 single crystal. The expansion of the Fermi arc is possibly attributed to a reduction in the tunnel barrier of the (Bi,Pb)–O block layer, where long-period crystallographic modulations are less pronounced [53].

5. Josephson Plasma Resonance and Terahertz Radiation

When considering superconducting electron pair tunneling in a single Josephson junction, the Hamiltonian with the number of tunneling electron pairs n and the gauge-invariant phase difference in the Josephson junction φ as conjugate variables is expressed as

$$\begin{aligned} H &= \frac{(2e)^2}{2C}n^2 + \frac{\hbar}{2e}J_c(1-\cos\varphi) \\ &\simeq \frac{(2e)^2}{2C}n^2 + \frac{\hbar}{4e}J_c\varphi^2, \end{aligned} \tag{3}$$

and is a harmonic oscillator within a linear approximation of the phase difference φ. In Eq. (3), C and J_c are the capacitance and the critical current density of the Josephson junction, respectively. The eigenfrequency of this harmonic oscillator is called the Josephson plasma frequency $\omega_p = \sqrt{8\pi edJ_c/\epsilon\hbar}$, where d is the thickness of the barrier layer of the Josephson junction, ϵ is the dielectric constant of the BL, and $\hbar$ is the Dirac constant. Since the Josephson plasma frequency is proportional to the square root of the Josephson maximum current J_c, the Josephson plasma frequency decreases with increasing magnetic field and temperature. In highly anisotropic bismuth-based high-T_c superconductors, $\omega_p/2\pi$ is located at approximately 100 GHz at absolute zero and zero magnetic field. Considering that the superconducting electron density depends on temperature according to the two-fluid model, the zero frequency limit is reach near T_c. At this intermediate temperature and a finite magnetic field, it absorbs electromagnetic waves in the millimeter wave range. This is called Josephson plasma resonance. Josephson plasma resonance in Bi2212 under magnetic fields was first reported by Matsuda et al. [6] as a means of observing its vortex state. As $\omega_p \propto \langle\cos\varphi_{l,l+1}\rangle$, cosine of the phase difference between adjacent superconducting layers averaged over the crystal. We discovered a sample-size-dependent transverse plasma mode [8] and its modulation by Josephson vortices [11]. Josephson plasma resonance is the inverse process of the terahertz electromagnetic radiation as discussed in the following sections. Both microwave irradiation and ac-Josephson effect under a voltage bias excite the phase collective mode. The former is dissipated as Joule heat, whereas the latter is emitted into space. The observed polarization of the radiated terahertz wave is determined by the boundary condition between the superconducting device and space; thus, the polarization and intensity are the results of the distributions of the superconducting current oscillating in the terahertz region.

6. Correlation between Temperature Distribution and Radiation Intensity

In the terahertz region, which lies between the frequencies of radio waves and light, no solid-state source with a practical intensity exceeding 1 mW was ever obtained. This is because the frequency is limited by the upper limit of the semiconductor mobility. Even when carrier dynamics are utilized, as in the microwave region, and even when quantum effects are utilized, as in LEDs, the energy is equivalent to a temperature of less than 50 K, and cryogenic temperatures are required. This is based on my understanding that The Josephson junction is expected to excite coherent electromagnetic waves with low dissipation in the order of tens of meV in the case of Bi2212, and that this is because the AC Josephson effect can convert DC voltage into AC current and the collective excitation around a few terahertz is protected by the superconducting gap [54]. The mechanism of terahertz radiation is that when electromagnetic waves excited by the AC Josephson effect match the resonance conditions of a cavity resonator consisting of Bi2212 single crystals, synchronous oscillations occur at the stacked IJJs [14]. In previous studies, radiation of monochromatic electromagnetic waves in the frequency range 0.3–1.6 THz with a maximum power of 0.6 mW has been reported [55]. As the high-temperature superconducting THz source operates at a finite voltage by injecting current into the superconductor, a problem has been pointed out that the temperature rise caused by Joule heating destroys the superconducting state and reduces the output power of the source.

To precisely compare the temperature distribution and radiation intensity depending on the current-injection conditions, we constructed an imaging system that could observe the temperature distribution on the device surface even in cryogenic environments below 100 K. This is an experimental technique used to observe the spatial distribution of fluorescence. This is achieved by applying a thin coating of a material containing rare earth elements called the Eu-TFC polymer, which shows a strong temperature dependence of fluorescence intensity on the device surface [56]. The device has two electrodes, so the temperature distribution and radiation intensity can be compared under non-uniform con-

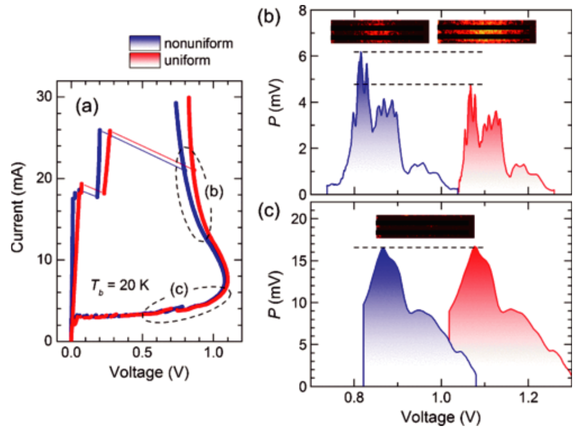

Fig. 4 (a) Current–voltage characteristics of the device. Oscillation occurs in the region enclosed by the dashed line. The difference between blue (non-uniform) and red (uniform) does not originate from the device. (b) Comparison of radiation intensity and temperature distribution in the high bias region. The oscillation intensity is lower in the uniform condition where the temperature rise is more pronounced. (c) Comparison in the low bias region. No difference is observed between the two. The voltages for the non-uniform case have offsets of 0.2 V in (b) and (c). Reproduced with permission from [35], copyright 2014 The American Physical Society.

ditions, in which the current is injected from one electrode, and under uniform conditions, in which the same amount of current is injected from both electrodes. As shown in Fig. 4, in the radiation region where the current value is around 20 mA, the temperature on the device surface is clearly higher under the uniform condition, and the area where the temperature exceeds T_c is larger. On the other hand, as shown in Fig. 4 (b), the radiation intensity is found to be approximately 20% weaker than in the non-uniform condition. As shown in Fig. 4 (c), there is no significant difference in both the temperature distribution and radiation intensity with a current value of approximately 5 mA. This result was reproduced in numerical simulations, which revealed that an excessive temperature rise on the device surface suppresses the radiation intensity [35]. This means that efficient cooling of the high-temperature superconducting THz source improves the radiation intensity, leading to the realization of high-power THz sources [57].

7. Circularly Polarized Terahertz Radiation

The polarization of terahertz radiation is of special importance in circular dichroism spectroscopy and high-speed telecommunications. Circularly polarized terahertz radiation has recently been achieved using monolithic devices, such as quantum cascade lasers and resonant-tunneling diodes. Compared to these devices, the Josephson plasma emitter can cover a wider frequency range in a single device, and other emission properties can be thermally controlled internally and externally. Circularly polarized electromagnetic waves have orthogonal components of the oscillating electric fields that are out of phase by 90 degrees, and the electric–field vector projected onto the propagation plane forms a circular orbit [58]. We have applied the patch

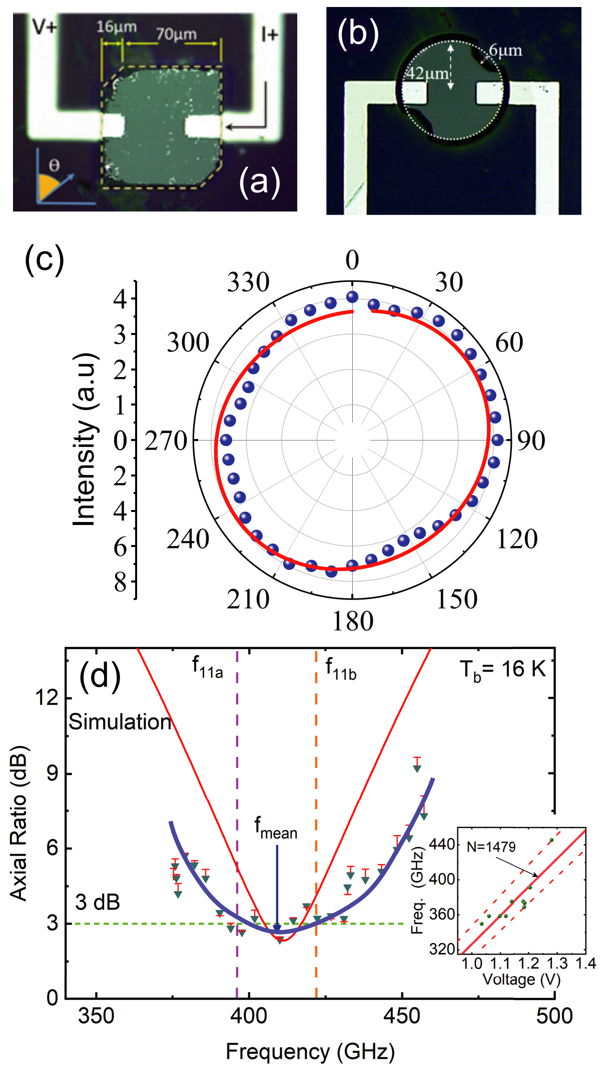

Fig. 5 (a, b) Pictures of the truncated edge square device (a) and the trimmed disk device (b). (c) Transmitted intensity of the rotating polarizer from the device shown in (b). (d) Measured axal ratio in the device shown in (c) as a function of radiation frequency (triangle). The solid red line is the expected axial ratio from the patch antenna model and the blue symbols are the experimental result is much broader than the patch antenna model. Inset of (d) shows measured frequency as a function of bias voltage, which is used to estimate the radiation frequencies from mesa voltages. Reproduced with permission from [37] and [38], copyright 2017 The American Physical Society and 2018 AIP Publishing LLC.

antenna theory for a high-temperature superconductor terahertz source to generate circularly polarized terahertz electromagnetic waves.

Figures 5 (a) and (b) show photographs of the mesa structures of Josephson plasma emitters designed with reference to the patch antenna theory and data on the polarization intensity characteristics under conditions of maximum circular polarization. One of the mesa structures is a square with truncated corners displayed in Fig. 5 (a), and circular polarization is radiated when the ratio of the area of the original square to the area of the corner part satisfies a specific relationship with respect to the Q-value of the antenna. The 99.7% circular polarization obtained in this study as observed in Fig. 5 (c) is the highest value compared to existing terahertz continuous sources, which adds another useful feature to the Josephson plasma emitter [37]. Cylindrical mesas with small notched sides (Fig. 5 (b)) also radiates terahertz waves with high degrees of circular polarization at wider frequency range than that expected by the conventional patch antenna theory as shown in Fig. 5 (d). This is presumably attributed to frequency locking (entrainment) due to strong interaction between the stacked IJJs [38].

As mentioned earlier, because the Josephson plasma emitter can vary its emission frequency widely, the degree of circular polarization depends on the bias conditions. While a conventional patch antenna is supplied with electromagnetic waves from an external source, the patch structure of the Josephson plasma emitter itself supplies the electromagnetic waves. The dependence of the degree of circular polarization on the bias condition provides insight into the internal excitation mode, thus, the synchronization mechanism. Circularly polarized terahertz waves are a useful technology for future applications in ultrafast mobile communications and circular dichroism spectroscopy; however, high degrees of circular polarization have not been achieved in monolithic devices.

8. Polarization Analysis of Synchronous Radiation

Synchronized terahertz radiation from multiple mesa structures has been attempted to achieve high radiation intensity in Josephson plasma emitters. It has been known that, by applying DC bias to multiple mesas formed on a Bi2212 crystal either parallel or series, macroscopic Josephson plasma oscillations excited in the mesas are synchronized. This results in a significant increase in radiation intensity, which is roughly proportional to the squared number of mesas. The maximum radiation intensity achieved by far is 0.61 mW in a device biased at three mesas in parallel [55]. However, the microscopic mechanism of coupling between mesas that leads to synchronized oscillations is poorly understood, making it extremely difficult to design high–intensity radiation. Therefore, we propose a method to estimate the state of Josephson plasma oscillation excited in the mesas from the polarization observation of the emitted terahertz wave. Moreover, this method also allows for elucidating the coupling mechanism through the superconducting single-crystal substrate underneath the mesas.

We observed the intensity, frequency, and polarization of terahertz waves emitted from two mesa structures formed on a single-crystal substrate for series- and parallel-connected simultaneous operations as shown in Fig. 6 (a). Polarization observations enable the estimation of the phase of the electromagnetic wave, which makes it possible to represent the radiation state as a vector. As a result, we showed that the radiation electric vector of simultaneous operation $\mathbf{E}_{A\|B} = \mathbf{E}^0_{A\|B}\exp(i\omega t)$ can be described by a linear combination based on the single operation of the two mesas $\mathbf{E}_A$ and $\mathbf{E}_B$ as

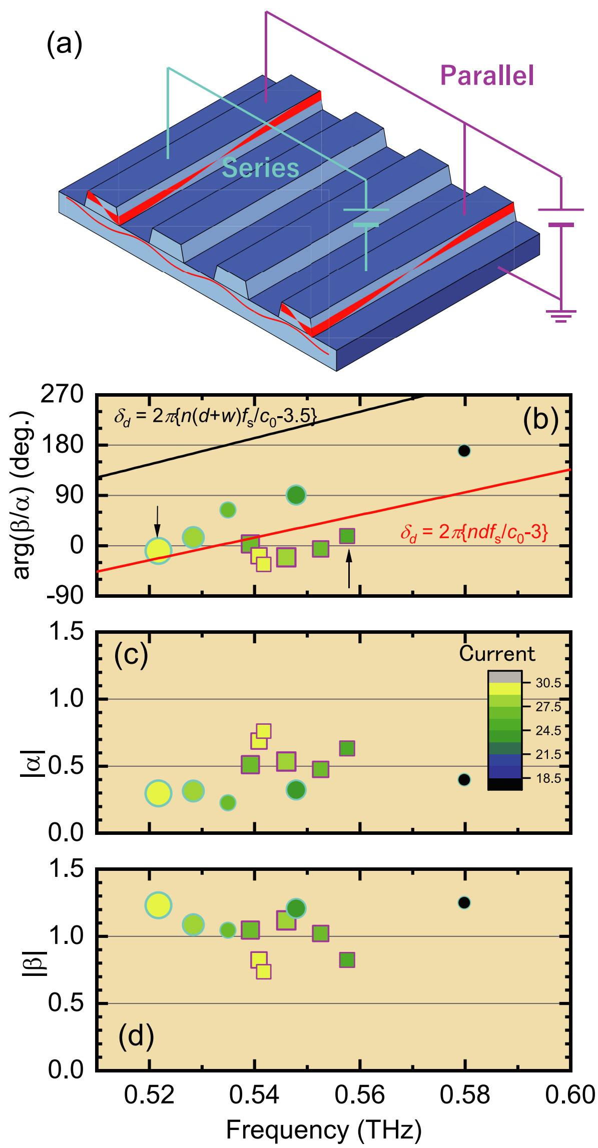

Fig. 6 (a) Schematic drawing of the device operated with parallel (purple) and series (cyan) connections. Red shadows indicate excited nonlinear Josephson plasma waves inside the mesas and a red wave indicates a linear Josephson plasma wave interacting with the mesas. (b) Phase difference of the coefficients α and β for parallel (square) and series (circle) connections as functions of synchronized frequency. Arrows point to data with the same basis frequencies selected. The solid black and red lines mean expected phase difference for the center-to-center and the nearer edge-to-edge distances of the mesas, respectively. (c,d) Absolute values of α and β. Both do not strongly depend on synchronized frequency. Symbol size means detected intensity of the synchronized radiations. Reproduced with permission from [40], copyright 2022 The American Physical Society.

$$\mathbf{E}_{A\|B} = \alpha\mathbf{E}_A + \beta\mathbf{E}_B, \tag{4}$$

where α and β are complex constants corresponding to interaction between the two mesas. This is because $\mathbf{E}_{A\|B}$ is not a superposition of bases $\mathbf{E}_A$ and $\mathbf{E}_B$ but accompanies frequency and phase shifts attributed to the inter-mesa couplings [39].

Figure 6 shows the frequency evolution of the coefficients α and β of a synchronized radiation in a device with two mesas connected either parallel (square) and series (circle). Here, two bases are fixed at the frequency indicated by an arrow either parallel and series and the phase difference of the base $\delta_\gamma = \arg(\beta/\alpha)$ linearly increase with synchronized frequency. Both of parallel and series connections show systematic evolutions in this frequency range. The solid lines describe expected phase differences from distance (edge-to-edge) and pitch (center-to-center) of the mesas [40].

Performing further analysis on the coefficients α and β under different experimental conditions such as inter-mesa separation and bath temperature, we can estimate the interaction matrix of Josephson plasma oscillations excited by the two mesa structures. This paves the way for the design of high intensity radiation devices, and also suggests the possibility of terahertz quantum communication devices.

9. Conclusion

The characteristic phenomena of intrinsic Josephson junctions, such as macroscopic quantum tunneling, intrinsic tunneling spectroscopy, and terahertz radiations, are discussed. These include a range of concepts physics, not only superconductivity but also interacting non-linear oscillator systems and quantum optics. Furthermore, elucidating their mechanisms makes it possible to control the performance of terahertz Josephson plasma emitters composed of intrinsic Josephson junction mesa structures. Thus this effort paved the way for implementing the physics of intrinsic Josephson junctions in practical telecommunication networks and imaging systems.

Acknowledgements

This study was supported by the Japan Society for the Promotion of Science (JSPS) KAKENHI (Grant No. JP20H02606) and the JSPS—Centre national de la recherche scientifique (CNRS) Bilateral Program (Grant No. JSPSBP120192908). The author thanks M. Suzuki, K. Kadowaki, T. Yamamoto, and M. Tsujimoto for their long-term close collaboration; H. Kambara, S. Komori, Y. Nomura, A. Elarabi, and R. Kobayashi for their significant efforts in determining the nature of IJJs, and M. Machida, T. Koyama, T. Kashiwagi, A. Koshelev, U. Welp, T. Benseman, H.B. Wang, R. Keiner, and S. Dhillon for stimulating discussions on intrinsic Josephson junctions and terahertz physics.

References

[1] R. Kleiner, F. Steinmeyer, G. Kunkel, and P. Müller, "Intrinsic Josephson effects in $Bi_2Sr_2CaCu_2O_8$ single crystals," Phys. Rev. Lett., vol.68, no.15, pp.2394–2397, 1992.

[2] G. Oya, N. Aoyama, A. Irie, S. Kishida, and H. Tokutaka, "Observation of Josephson Junctionlike Behavior in Single-Crystal (Bi, Pb)$_2Sr_2CaCu_2O_y$," Jpn. J. Appl. Phys., vol.31, Part 2, no.7A, pp.L829–L831, July 1992.

[3] R. Kleiner and P. Müller, "Intrinsic Josephson effects in high-T_c superconductors," Phys. Rev. B, vol.49, no.2, pp.1327–1341, Jan. 1994.

[4] M. Suzuki, T. Watanabe, and A. Matsuda, "Interlayer Tunneling Spectroscopy for Slightly Overdoped $Bi_2Sr_2CaCu_2O_{8+\delta}$," Phys. Rev. Lett., vol.82, no.26, pp.5361–5364, June 1999.

[5] V.M. Krasnov, A. Yurgens, D. Winkler, P. Delsing, and T. Claeson, "Evidence for coexistence of the superconducting gap and pseudogap in Bi-2212 from intrinsic tunneling spectroscopy," Phys. Rev. Lett., vol.84, no.25, p.5860, 2000.

[6] Y. Matsuda, M. Gaifullin, K. Kumagai, K. Kadowaki, and T. Mochiku, "Collective Josephson Plasma Resonance in the Vortex State of $Bi_2Sr_2CaCu_2O_{8+\delta}$," Phys. Rev. Lett., vol.75, no.24, pp.4512–4515, 1995.

[7] K. Kadowaki and I. Kakeya, "Longitudinal Josephson-plasma excitation in $Bi_2Sr_2CaCu_2O_{8+\delta}$: Direct observation of the Nambu-Goldstone mode in a superconductor," Phys. Rev. B - Condens. Matter Mater. Phys., vol.56, no.9, pp.5617–5621, 1997.

[8] I. Kakeya, K. Kindo, K. Kadowaki, S. Takahashi, and T. Mochiku, "Mode separation of the Josephson plasma in $Bi_2Sr_2CaCu_2O_{8+\delta}$," Phys. Rev. B, vol.57, no.5, pp.3108–3115, Feb. 1998.

[9] G. Hechtfischer, R. Kleiner, K. Schlenga, W. Walkenhorst, P. Müller, and H.L. Johnson, "Collective motion of Josephson vortices in intrinsic Josephson junctions in $Bi_2Sr_2CaCu_2O_{8+y}$," Phys. Rev. B, vol.55, no.21, pp.14638–14644, June 1997.

[10] S. Ooi, T. Mochiku, and K. Hirata, "Periodic Oscillations of Josephson-Vortex Flow Resistance in $Bi_2Sr_2CaCu_2O_{8+\delta}$," Phys. Rev. Lett., vol.89, no.24, p.247002, Nov. 2002.

[11] I. Kakeya, T. Wada, R. Nakamura, and K. Kadowaki, "Two phase collective modes in a Josephson vortex lattice in the intrinsic Josephson junction $Bi_2Sr_2CaCu_2O_{8+\delta}$," Phys. Rev. B - Condens. Matter Mater. Phys., vol.72, no.1, pp.14540–14541, 2005.

[12] I. Kakeya, Y. Kubo, M. Kohri, M. Iwase, T. Yamamoto, and K. Kadowaki, "Scaling behavior of the crossover to short-stack regimes of Josephson vortex lattices in $Bi_2Sr_2CaCu_2O_{8+\delta}$ stacks," Phys. Rev. B - Condens. Matter Mater. Phys., vol.79, no.21, p.212503, June 2009.

[13] A.E. Koshelev, A.I. Buzdin, I. Kakeya, T. Yamamoto, and K. Kadowaki, "Fluctuating pancake vortices revealed by dissipation of the Josephson vortex lattice," Phys. Rev. B - Condens. Matter Mater. Phys., vol.83, no.22, p.224515, June 2011.

[14] L. Ozyuzer, A.E. Koshelev, C. Kurter, N. Gopalsami, Q. Li, M. Tachiki, K. Kadowaki, T. Yamamoto, H. Minami, H. Yamaguchi, T. Tachiki, K.E. Gray, W.-K. Kwok, and U. Welp, "Emission of Coherent THz Radiation from Superconductors," Science, vol.318, no.5854, pp.1291–1293, Nov. 2007.

[15] X. Hu and S.-Z. Lin, "Phase dynamics in a stack of inductively coupled intrinsic Josephson junctions and terahertz electromagnetic radiation," Supercond. Sci. Technol., vol.23, no.5, p.053001, May 2010.

[16] U. Welp, K. Kadowaki, and R. Kleiner, "Superconducting emitters of THz radiation," Nat. Photonics, vol.7, no.9, pp.702–710, Aug. 2013.

[17] I. Kakeya and H. Wang, "Terahertz-wave emission from Bi2212 intrinsic Josephson junctions: a review on recent progress," Supercond. Sci. Technol., vol.29, no.7, p.073001, 2016.

[18] T. Kashiwagi, H. Kubo, K. Sakamoto, T. Yuasa, Y. Tanabe, C. Watanabe, T. Tanaka, Y. Komori, R. Ota, G. Kuwano, K. Nakamura, T. Katsuragawa, M. Tsujimoto, T. Yamamoto, R. Yoshizaki, H. Minami, K. Kadowaki, and R.A. Klemm, "The present status of high-T_c superconducting terahertz emitters," Supercond. Sci. Technol., vol.30, no.7, p.074008, July 2017.

[19] R. Kleiner and H. Wang, "Terahertz emission from $Bi_2Sr_2CaCu_2O_{8+x}$ intrinsic Josephson junction stacks," J. Appl. Phys., vol.126, no.17, p.171101, Nov. 2019.

[20] M. Machida, T. Koyama, A. Tanaka, and M. Tachiki, "Collective dynamics of Josephson vortices in intrinsic Josephson junctions: Exploration of in-phase locked superradiant vortex flow states," Phys.

C Supercond. its Appl., vol.330, no.1-2, pp.85–93, 2000.

[21] T.M. Benseman, A.E. Koshelev, K.E. Gray, W.K. Kwok, U. Welp, K. Kadowaki, M. Tachiki, and T. Yamamoto, "Tunable terahertz emission from $Bi_2Sr_2CaCu_2O_{8+\delta}$ mesa devices," Phys. Rev. B, vol.84, no.6, p.064523, Aug. 2011.

[22] T. Tachiki, H. Katada, and T. Uchida, "Evaluation of cavity modes in superconducting intrinsic-josephson-junction oscillators for terahertz-wave generation," J. Infrared, Millimeter, Terahertz Waves, vol.35, no.6-7, pp.509–516, 2014.

[23] E.A. Borodianskyi and V.M. Krasnov, "Josephson emission with frequency span 1–11 THz from small $Bi_2Sr_2CaCu_2O_{8+\delta}$ mesa structures," Nat. Commun., vol.8, no.1, p.1742, Dec. 2017.

[24] T. Uchida, W. Kimura, K. Nakajima, T. Tachiki, and T. Uchida, "Effect of RF Isolation of Intrinsic Josephson Junctions Made of Solid Bi-2212 Film for Terahertz Radiation," IEEE Trans. Appl. Supercond., vol.28, no.4, 1800304, 2018.

[25] Y. Saito, I. Kakeya, and Y. Takano, "Polarization analysis of terahertz emission from Bi-2212 cross-whisker intrinsic Josephson junction devices and their refractive index," Appl. Phys. Lett., vol.121, no.21, p.212601, Nov. 2022.

[26] S. Sakai, P. Bodin, and N.F. Pedersen, "Fluxons in thin-film superconductor-insulator superlattices," J. Appl. Phys., vol.73, no.5, pp.2411–2418, March 1993.

[27] T. Koyama and M. Tachiki, "*I-V* characteristics of Josephson-coupled layered superconductors with longitudinal plasma excitations," Phys. Rev. B, vol.54, no.22, p.16183, 1996.

[28] M. Machida, T. Koyama, and M. Tachiki, "Dynamical Breaking of Charge Neutrality in Intrinsic Josephson Junctions: Common Origin for Microwave Resonant Absorptions and Multiple-Branch Structures in the *I-V* Characteristics," Phys. Rev. Lett., vol.83, no.22, pp.4618–4621, Nov. 1999.

[29] H. Kambara, I. Kakeya, and M. Suzuki, "Increase of superfluid density with growth of quasiparticle density of states probed by intrinsic tunneling spectroscopy in $Bi_{1.9}Pb_{0.1}Sr_2CaCu_2O_{8+\delta}$," Phys. Rev. B - Condens. Matter Mater. Phys., vol.87, no.21, 2013.

[30] S. Komori and I. Kakeya, "Interlayer Transport and Josephson Coupling in a 1212-type Cuprate Superconductor with a (Pb,Cu)-O Barrier Layer," J. Phys. Soc. Japan, vol.90, no.2, 2021.

[31] Y. Nomura, T. Mizuno, H. Kambara, Y. Nakagawa, and I. Kakeya, "Enhanced Macroscopic Quantum Tunneling in Capacitively Coupled BiPb2201 Single-Layered Intrinsic Josephson Junctions," J. Phys. Soc. Japan, vol.84, no.1, p.013704, Jan. 2015.

[32] Y. Nomura, R. Okamoto, and I. Kakeya, "Negative correlation between enhanced crossover temperature and fluctuation-free critical current of the second switch in $Bi_2Sr_2CaCu_2O_{8+\delta}$ intrinsic Josephson junction," Supercond. Sci. Technol., vol.30, no.10, p.105001, Oct. 2017.

[33] Y. Nomura, R. Okamoto, T.A. Mizuno, S. Adachi, T. Watanabe, M. Suzuki, and I. Kakeya, "Role of the inner copper oxide plane in interlayer Josephson effects in multilayered cuprate superconductors," Phys. Rev. B, vol.100, no.14, p.144515, Oct. 2019.

[34] I. Kakeya, Y. Omukai, T. Yamamoto, K. Kadowaki, and M. Suzuki, "Effect of thermal inhomogeneity for terahertz radiation from intrinsic Josephson junction stacks of $Bi_2Sr_2CaCu_2O_{8+\delta}$," Appl. Phys. Lett., vol.100, no.24, p.242603, June 2012.

[35] M. Tsujimoto, H. Kambara, Y. Maeda, Y. Yoshioka, Y. Nakagawa, and I. Kakeya, "Dynamic Control of Temperature Distributions in Stacks of Intrinsic Josephson Junctions in $Bi_2Sr_2CaCu_2O_{8+\delta}$ for Intense Terahertz Radiation," Phys. Rev. Appl., vol.2, no.4, p.044016, Oct. 2014.

[36] I. Kakeya, N. Hirayama, Y. Omukai, and M. Suzuki, "Temperature dependence of terahertz emission by an asymmetric intrinsic Josephson junction device," J. Appl. Phys., vol.117, no.4, p.043914, 2015.

[37] A. Elarabi, Y. Yoshioka, M. Tsujimoto, and I. Kakeya, "Monolithic Superconducting Emitter of Tunable Circularly Polarized Terahertz Radiation," Phys. Rev. Appl., vol.8, no.6, p.064034, Dec. 2017.

[38] A. Elarabi, Y. Yoshioka, M. Tsujimoto, and I. Kakeya, "Circularly polarized terahertz radiation monolithically generated by cylindrical mesas of intrinsic Josephson junctions," Appl. Phys. Lett., vol.113, no.5, p.052601, July 2018.

[39] M. Tsujimoto, S. Fujita, G. Kuwano, K. Maeda, A. Elarabi, J. Hawecker, J. Tignon, J. Mangeney, S.S. Dhillon, and I. Kakeya, "Mutually Synchronized Macroscopic Josephson Oscillations Demonstrated by Polarization Analysis of Superconducting Terahertz Emitters," Phys. Rev. Appl., vol.13, no.5, p.051001, May 2020.

[40] R. Kobayashi, K. Hayama, S. Fujita, M. Tsujimoto, and I. Kakeya, "Spontaneous Frequency Shift and Phase Delay of Coupled Terahertz Radiation Mediated by the Josephson Plasmon in a Cuprate Superconductor," Phys. Rev. Appl., vol.17, no.5, p.054043, May 2022.

[41] K. Inomata, S. Sato, K. Nakajima, A. Tanaka, Y. Takano, H.B. Wang, M. Nagao, H. Hatano, and S. Kawabata, "Macroscopic Quantum Tunneling in a d-Wave High-T_c $Bi_2Sr_2CaCu_2O_{8+\delta}$ Superconductor," Phys. Rev. Lett., vol.95, no.10, p.107005, Sept. 2005.

[42] X.Y. Jin, J. Lisenfeld, Y. Koval, A. Lukashenko, A.V. Ustinov, and P. Müller, "Enhanced Macroscopic Quantum Tunneling in $Bi_2Sr_2CaCu_2O_{8+\delta}$ Intrinsic Josephson-Junction Stacks," Phys. Rev. Lett., vol.96, no.17, p.177003, May 2006.

[43] S.-X. Li, W. Qiu, S. Han, Y.F. Wei, X.B. Zhu, C.Z. Gu, S.P. Zhao, and H.B. Wang, "Observation of Macroscopic Quantum Tunneling in a Single $Bi_2Sr_2CaCu_2O_{8+\delta}$ Surface Intrinsic Josephson Junction," Phys. Rev. Lett., vol.99, no.3, p.037002, July 2007.

[44] H. Kashiwaya, T. Matsumoto, H. Shibata, S. Kashiwaya, H. Eisaki, Y. Yoshida, S. Kawabata, and Y. Tanaka, "Switching Dynamics of $Bi_2Sr_2CaCu_2O_{8+\delta}$ Intrinsic Josephson Junctions: Macroscopic Quantum Tunneling and Self-Heating Effect," J. Phys. Soc. Japan, vol.77, no.10, p.104708, Oct. 2008.

[45] K. Ota, K. Hamada, R. Takemura, M. Ohmaki, T. Machi, K. Tanabe, M. Suzuki, A. Maeda, and H. Kitano, "Comparative study of macroscopic quantum tunneling in $Bi_2Sr_2CaCu_2O_y$ intrinsic Josephson junctions with different device structures," Phys. Rev. B, vol.79, no.13, p.134505, April 2009.

[46] Y. Kubo, Y. Takahide, S. Ueda, Y. Takano, and Y. Ootuka, "Macroscopic Quantum Tunneling in a $Bi_2Sr_2CaCu_2O_{8+\delta}$ Single Crystalline Whisker," Appl. Phys. Express, vol.3, no.6, p.063104, June 2010.

[47] A. Yamaguchi, H. Ohnuma, Y. Watabe, S. Umegai, K. Hosaka, and H. Kitano, "Comparative Study of First and Second Switches with Nearly Identical Switching Current in $Bi_2Sr_2Ca_{0.85}Y_{0.15}Cu_2O_y$ Intrinsic Josephson Junctions," J. Phys. Soc. Japan, vol.88, no.10, p.103704, Oct. 2019.

[48] I. Kakeya, K. Hamada, T. Tachiki, T. Watanabe, and M. Suzuki, "Switching current distributions and macroscopic quantum tunneling in over-doped BSCCO mesas with nanometer thickness," Supercond. Sci. Technol., vol.22, no.11, p.114014, Nov. 2009.

[49] H.A. Kramers, "Brownian motion in a field of force and the diffusion model of chemical reactions," Physica, vol.7, no.4, pp.284–304, April 1940.

[50] V. Ambegaokar and A. Baratoff, "Tunneling Between Superconductors," Phys. Rev. Lett., vol.11, no.2, p.104, July 1963.

[51] A. Kanigel, M.R. Norman, M. Randeria, U. Chatterjee, S. Souma, A. Kaminski, H.M. Fretwell, S. Rosenkranz, M. Shi, T. Sato, T. Takahashi, Z.Z. Li, H. Raffy, K. Kadowaki, D. Hinks, L. Ozyuzer, and J.C. Campuzano, "Evolution of the pseudogap from Fermi arcs to the nodal liquid," Nat. Phys., vol.2, pp.447–451, 2006.

[52] M. Suzuki, R. Takemura, K. Hamada, M. Ohmaki, and T. Watanabe, "Short-Pulse Intrinsic Tunneling Spectroscopy in $Bi_2Sr_2CaCu_2O_{8+\delta}$ under Suppressed Self Heating," Jpn. J. Appl. Phys., vol.51, no.1R, p.010112, Jan. 2012.

[53] R. Gladyshevskii, N. Musolino, and R. Flükiger, "Structural origin of the low superconducting anisotropy of $Bi_{1.7}Sr_{0.4}Ca_{0.9}Cu_2O_8$ crystals," Phys. Rev. B, vol.70, no.18, p.184522, Nov. 2004.

[54] M. Tachiki, T. Koyama, and S. Takahashi, "Electromagnetic phe-

nomena related to a low-frequency plasma in cuprate superconductors," Phys. Rev. B, vol.50, no.10, pp.7065–7084, 1994.

[55] T.M. Benseman, K.E. Gray, A.E. Koshelev, W.-K. Kwok, U. Welp, H. Minami, K. Kadowaki, and T. Yamamoto, "Powerful terahertz emission from $Bi_2Sr_2CaCu_2O_{8+\delta}$ mesa arrays," Appl. Phys. Lett., vol.103, no.2, p.022602, 2013.

[56] H.B. Wang, S. Guénon, J. Yuan, A. Iishi, S. Arisawa, T. Hatano, T. Yamashita, D. Koelle, and R. Kleiner, "Hot spots and waves in $Bi_2Sr_2CaCu_2O_8$ intrinsic Josephson junction stacks: A study by low temperature scanning laser microscopy," Phys. Rev. Lett., vol.102, no.1, p.17006, 2009.

[57] M. Tsujimoto, T. Doi, G. Kuwano, A. Elarabi, and I. Kakeya, "Engineering and characterization of a packaged high-T_c superconducting terahertz source module," Supercond. Sci. Technol., vol.30, no.6, p.064001, June 2017.

[58] C.A. Balanis, Antenna Theory: Analysis and Design, 4th Edition, John Wiley & Sons, 2015.

Itsuhiro Kakeya received the B.S., M.S., and PhD. degrees in Physics from Osaka University in 1994, 1996, and 1998 respectively. During 1998–2008, he had been an assistant professor and a lecturer of University of Tsukuba. He has been an associate professor of Kyoto University since 2008. He was also appointed as a visiting professor of École normale supérieuer (ENS)-PSL, France at 2017.